Nanoscale

PAPER

View Article Online
View Journal | View Issue

Cite this: *Nanoscale*, 2024, **16**, 4637

Carbon dot enhanced peroxidase-like activity of platinum nanozymes†

Cui Liu, [a] Jiao Hu, [b] Wenwen Yang,[c,d] Jinyu Shi,[a,e] Yiming Chen,[f] Xing Fan,[g] Wenhui Gao,[f] Liangliang Cheng,[f] Qing-Ying Luo *[c] and Mingzhen Zhang *[f]

Received 3rd October 2023,
Accepted 15th January 2024

DOI: 10.1039/d3nr04964g

rsc.li/nanoscale

As one of the most intriguing nanozymes, the platinum (Pt) nanozyme has attracted tremendous research interest due to its various catalytic activities but its application is still limited by its poor colloidal stability and low affinity to substrates. Here, we design a highly stable Pt@carbon dot (Pt@CD) hybrid nanozyme with enhanced peroxidase (POD)-like activity (specific activity of 1877 U mg^{-1}). The Pt@CDs catalyze the decomposition of hydrogen peroxide (H_2O_2) to produce singlet oxygen and hydroxyl radicals and exhibit high affinity to H_2O_2 and high specificity to 3,3′,5,5′-tetramethyl-benzidine. We reveal that both the hydroxyl and carbonyl groups of CDs could coordinate with Pt^{2+} and then regulate the charge state of the Pt nanozyme, facilitating the formation of Pt@CDs and improving the POD-like activity of Pt@CDs. Colorimetric detection assays based on Pt@CDs for H_2O_2, dopamine, and glucose with a satisfactory detection performance are achieved. Moreover, the Pt@CDs show a H_2O_2-involving antibacterial effect by destroying the cell membrane. Our findings provide new opportunities for designing hybrid nanozymes with desirable stability and catalytic performance by using CDs as nucleating templates and stabilizers.

Introduction

Enzymes, powerful biocatalysts, play essential roles in nearly all cellular metabolic processes and have extensive applications in medical, industrial, and biological domains owing to their superior catalytic efficiency and specific substrate recognition.[1–4] Nevertheless, inherent limitations such as expensive production, limited stability, vulnerable catalytic activity, and difficulties in recovery and reuse of natural enzymes have greatly hindered their applications.[5] To overcome these limitations, artificial enzymes have been vigorously explored. Since the discovery of peroxidase (POD)-like activity in Fe_3O_4 nanoparticles by Yan *et al.*,[6] many studies on nanomaterials with enzyme-like activities (nanozymes) have emerged.[7–12] Nanozymes offer several advantages over natural enzymes, including high stability, durability, low cost,[13–15] and great potential in biosensing,[16–18] environmental treatment,[19,20] therapeutics,[21–23] antibacterial treatment,[24,25] and cellular protection.[26–28] As one of the most attractive nanozymes, the Pt nanozyme has various catalytic activities, such as POD, catalase (CAT), and superoxide-like activities.[29–31] Generally, the smaller the size, the more the catalytic sites present on the surface of nanozymes. However, small particle size-enhanced surface free energy makes Pt nanoparticles (PtNPs) easy to aggregate and lose their catalytic activity. Dendrimers,[32] polymers (like polydopamine, polyvinylpyrrolidone (PVP)),[33] proteins,[34–37] DNA,[38] and small molecules[39,40] have been employed to coat PtNPs for enhancing their stability. Nonetheless, stabilizers or capping molecules also obstruct the catalytically active sites located on the surface of PtNPs, resulting in the decline in catalytic activity.[34] Promoting both the catalytic activity and the colloidal stability of Pt-based nanozymes still remains a great challenge.

The design of hybrid nanozymes provides an effective approach to overcome the challenges mentioned above. Carbon nanomaterials have been extensively utilized to prepare hybrid nanozymes owing to their excellent electronic conductivity, favourable biocompatibility, stable chemical properties, and convenient surface functionalization. For

[a]*Chongqing Key Laboratory of Natural Product Synthesis and Drug Research, Innovative Drug Research Center, School of Pharmaceutical Sciences, Chongqing University, Chongqing, 400044, P. R. China*
[b]*Hubei Key Laboratory of Environmental and Health Effects of Persistent Toxic Substances, School of Environment and Health, Jianghan University, Wuhan, 430056, P. R. China*
[c]*School of Food and Drug, Shenzhen Polytechnic University, Shenzhen 518055, P. R. China. E-mail: Luoqingying@szpu.edu.cn*
[d]*School of Life Sciences, Guizhou Normal University, Guiyang 550025, P. R. China*
[e]*School of Chemical Science and Technology, Yunnan University, Kunming, 650500, P.R. China*
[f]*School of Basic Medical Sciences, Xi'an Key Laboratory of Immune Related Diseases, Xi'an Jiaotong University Health Science Center, Xi'an, Shaanxi, 710061, P. R. China. E-mail: mzhang21@xjtu.edu.cn*
[g]*Department of Pathology, the First Affiliated Hospital of Xi'an Jiaotong University, Xi'an, Shaanxi, 710061, China*

†Electronic supplementary information (ESI) available. See DOI: https://doi.org/10.1039/d3nr04964g

example, graphene oxide–Fe_3O_4 nanozyme showed high POD-like activity with enhanced affinity for hydrogen peroxide (H_2O_2).[41] Qu's group reported a gold cluster–graphene hybrid with high POD-like activity in a broad pH range.[42] Furthermore, PtNPs dispersed on polymerized ionic liquid wrapped carbon nanotubes exhibited good stability and high catalytic activity.[43] Carbon dots (CDs), as a kind of zero-dimensional nanomaterial, have distinctive properties including high stability, environmental friendliness, easy preparation, and low cost.[44–47] Compared to graphene oxide, graphene, and carbon nanotubes, CDs have a smaller size, larger specific surface area, and more surface functional groups, which endow CDs with better potential to combine and stabilize metal nanoparticles. Therefore, PtNPs might grow on the CD surface through coordination with oxygen-containing groups of CDs, and then generate the Pt@CD hybrid nanozyme as a result. Notably, this hybrid system comprises only CDs and PtNPs, eliminating the requirement for extra linkers, stabilizers, or capping molecules. In this case, the catalytically active sites of PtNPs could be fully exposed. Due to the direct interaction between the CDs and the PtNPs, the electron transfer between them can effectively improve the enzymatic activity of the PtNPs. In our previous work,[48] we revealed that CDs can enhance Pt nanozymes' CAT-like activity. However, whether CDs can improve Pt nanozymes' POD-like activity remains unclear.

Herein, through the combination between CDs and Pt ions, Pt(IV) was reduced *in situ* on the surface of CDs with $NaBH_4$ (Scheme 1), generating a hybrid nanozyme, Pt@CD. As expected, the Pt@CDs exhibited good POD-like activity with a high specific activity of 1877 U mg^{-1}, high affinity to H_2O_2, and good specificity to 3,3′,5,5′-tetramethyl-benzidine (TMB). Based on Pt@CDs, a highly sensitive detection of H_2O_2 was achieved. The limit of detection (LOD) for H_2O_2 (3.27 μM) was significantly lower than the maximum allowable concentration of H_2O_2 according to US FDA, indicating that Pt@CDs can be utilized for H_2O_2 detection in dairy food products.

Cui Liu

Dr Cui Liu obtained her Ph.D. in analytical chemistry at Wuhan University in 2017. She is currently an associate professor at Chongqing University. Her research focuses on the synthesis, functionalization, catalytic mechanism, and applications of carbon dot nanozymes. Dr Liu serves as an academic editor of Exploration. *She has published >30 journal papers in* Nat. Commun., Angew. Chem., Adv. Funct. Mater., Nano Today *and other leading journals with >2000 citations.*

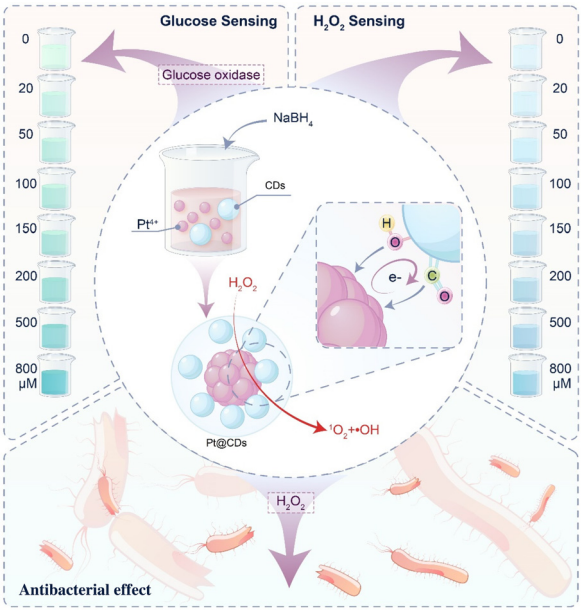

Scheme 1 Schematic representation of the synthesis and applications of Pt@CDs with enhanced POD-like activity.

Furthermore, due to the reducibility of dopamine (DA), a sensitive detection for DA with a LOD of 0.31 μM and a linear range of 1–100 μM was achieved. Furthermore, combining Pt@CDs with glucose oxidase (GOx), we established a highly sensitive glucose-detection assay, producing a LOD of 4.52 μM and a linear range of 10–800 μM. In addition, the antibacterial experiments demonstrated that a more potent bactericidal effect can be achieved by utilizing Pt@CDs at a lower concentration of H_2O_2.

Results and discussion

The CDs were prepared by using our previous reported method, in which carbon fiber powder was employed as the carbon source while a mixture acid ($V_{\text{nitric acid}}$: $V_{\text{sulfuric acid}}$ = 2 : 1) was used as the oxidizing agent.[49,50] They have a small size of approximately 2 nm and exhibited good monodispersity (Fig. 1a). From high-resolution transmission electron microscopy (HR-TEM) images, the lattice spacing of CDs was determined to be 0.21 nm, indicating the presence of the (100) facet of graphite. The synthesis of the Pt@CD nanocomposite involved the reduction of $PtCl_6^{2-}$ using $NaBH_4$ in the presence of CDs under alkaline conditions, in which CDs could combine with PtNPs through oxygen-containing groups. Due to this weak interaction between PtNPs and oxygen-containing groups upon the surface of CDs, the PtNPs exhibited a random morphology and a relatively wide size distribution of 5–10 nm (Fig. 1b). Precisely due to this weak interaction, the catalytic sites on the surface of the PtNPs can be fully exposed. The Pt@CDs possessed two lattices of 0.21 and 0.23 nm, attributed to the CDs and Pt (111) facets, respectively (Fig. 1c). Obviously,

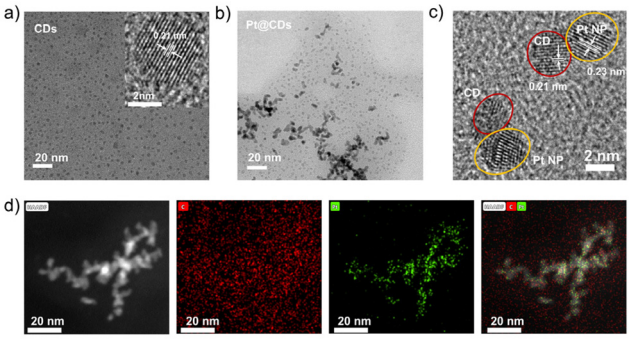

Fig. 1 TEM images of CDs (a) and Pt@CDs (b); the HR-TEM image of Pt@CDs (c). HAADF-STEM image and elemental mapping images of Pt@CDs (d).

the CDs were in excess compared with Pt NPs. However, upon removal of the excess free CDs, the stability of Pt@CDs decreased, leading to easy precipitation, which indicated that CDs also acted as stabilizers. The high-angle annular dark field scanning transmission electron microscopy (HAADF-STEM) and corresponding elemental mapping images of Pt@CDs (Fig. 1d) were further analyzed. It is evident that some of C and Pt elements overlay, while more of them are adjoining to each other, suggesting that the PtNPs grow on the surface of CDs and confirming the successful formation of the Pt@CD nanocomposite. The zeta potential of Pt@CDs was −24.8 mV (Fig. S1†), suggesting their high colloidal stability. In the absence of CDs, $NaBH_4$ reduced H_2PtCl_6 to form aggregate precipitates of PtNPs (Fig. S2 and 3†). In contrast, Pt@CDs solution exhibited as auniform brownish–black color and demostrated long-term stability for at least one year. Although PVP is often used as a capping molecule to enhance the stability of metal nanoparticles, when the PtNPs were prepared by replacing CDs with PVP in the same dose (1.6 mg), black precipitates appeared too (PVP capped PtNPs, named as PtNPs-PVP, Fig. S3†), indicating that CDs could stabilize PtNPs better than PVP probably due to more coordination sites on the surface of CDs.

The POD-like activity of Pt@CDs was investigated. As shown in Fig. 2a, with H_2O_2, the oxidation of TMB catalyzed by Pt@CDs leads to the formation of oxidized TMB (Ox-TMB) with absorbance peaks at 368 and 652 nm. Although the Pt@CDs have the ability to mimic oxidase to catalyze TMB oxidation by dissolved oxygen, the oxidase-like activity was very weak, leading to very light blue color. With H_2O_2, the oxidation of TMB catalyzed by Pt@CDs was more sufficient with an obvious blue color as a result, indicating the dominant POD-like activity of Pt@CDs. Compared with the individual CDs, PtNPs, or PtNPs-PVP at the same concentration, the Pt@CDs showed enhanced POD-like activity (Fig. S4†). Moreover, we also prepared PVP stabilized PtNPs by using the traditional method reported by Xia's group,[51] in which PVP serves as a stabilizer while ethylene glycol (EG) serves as both the reducing agent and the solvent, and the resulting sample was named PtNPs-PVP-EG. Different from PtNPs-PVP, the PtNPs-PVP-EG exhibited better dispersibility and stability due to the high dose of PVP (5 mg mL^{-1}). The catalytic performance of Pt@CDs was compared with that of PtNPs-PVP-EG at the same concentration. As shown in Fig. S5,† in the absence of H_2O_2, PtNPs-PVP-EG could catalyze the oxidation of TMB, suggesting that it can mimic oxidase. When H_2O_2 (1 mM) was introduced, there was a slight increase in the degree of TMB oxidation, with the absorbance at 652 nm increasing from 0.35 to 0.45. This indicated that PtNPs-PVP-EG mainly exhibited oxidase-like activity rather than POD-like activity. Nevertheless, the absorbance at 652 nm of the mixture containing Pt@CDs and TMB without and with H_2O_2 was 0.18 and 0.89, respectively, indicating their much higher POD-like activity than PtNPs-PVP-EG. These results indicated that combining with CDs could enhance both the colloidal stability and POD-like activity of PtNPs.

Based on their intrinsic POD-like activity, Pt-based nanozymes have been used in biosensing, environmental protection, antibacterial treatment, and cancer therapy.[1] Previous works have reported that the Pt nanozyme demonstrates its capability to catalyse the oxidation of TMB, 3,3′-diaminobenzidine (DAB), 2,2′-azinobis (3-ethylbenzothiazoline-6-sulfonic acid) (ABTS), or *o*-phenylenediamine (OPD) by H_2O_2 to produce colorimetric reactions.[52,53] However, the Pt@CDs can hardly catalyse the oxidation of ABTS, DAB, or OPD (Fig. S6†), showing the high substrate selectivity toward TMB. The reaction kinetics of the catalysis reaction was investigated at 652 nm due to the absorption of Ox-TMB. It was obvious that the catalytic activity of Pt@CDs was superior to that of PtNPs, PtNPs-PVP, and PtNPs-PVP-EG (Fig. S7†). To further confirm the enhanced catalytic activity of Pt@CDs, their Michaelis–Menten constant (K_m) reflecting the binding affinity between enzyme and substrate was acquired from the Lineweaver–Burk plot (Fig. 2c–f). The K_m value of Pt@CDs was estimated to be 61.1 μM for TMB, which is a seventh of the natural horseradish peroxidase (HRP, 0.434×10^{-3} M) (Table S1†), indicating their higher affinity to TMB due to the coordination between Pt and the amino groups of TMB, and the electrostatic/hydrogen bonding interaction between CDs and TMB. Although the K_m value of Pt@CDs (26.5 mM) for H_2O_2 was 7 times greater than that of HRP, the V_{max} value of Pt@CDs was much higher compared to that of HRP, indicating that Pt@CDs catalyze more H_2O_2 (0.91 mM) per second.

Many capping molecules including protein, PVP, DNA, and small molecules have been exploited to enhance the catalytic performance and colloidal stability of PtNPs. As shown in Table S1,† a high affinity to TMB could be easily obtained but the affinity to H_2O_2 is typically low. Increasing the affinity for H_2O_2 often results in a decrease in the affinity for TMB. For instance, Li *et al.*[54] reported that as the size of DNA capped PtNPs increased from 1.8 to 2.9 nm, the K_m for H_2O_2 decreased from 117.2 to 48 mM while that for TMB increased from 16.2 to 56 μM. It is of note that Pt@CDs not only showed high specificity and affinity to TMB, but also exhibited much higher affinity toward H_2O_2, (Table S1†), revealing that CDs play a key

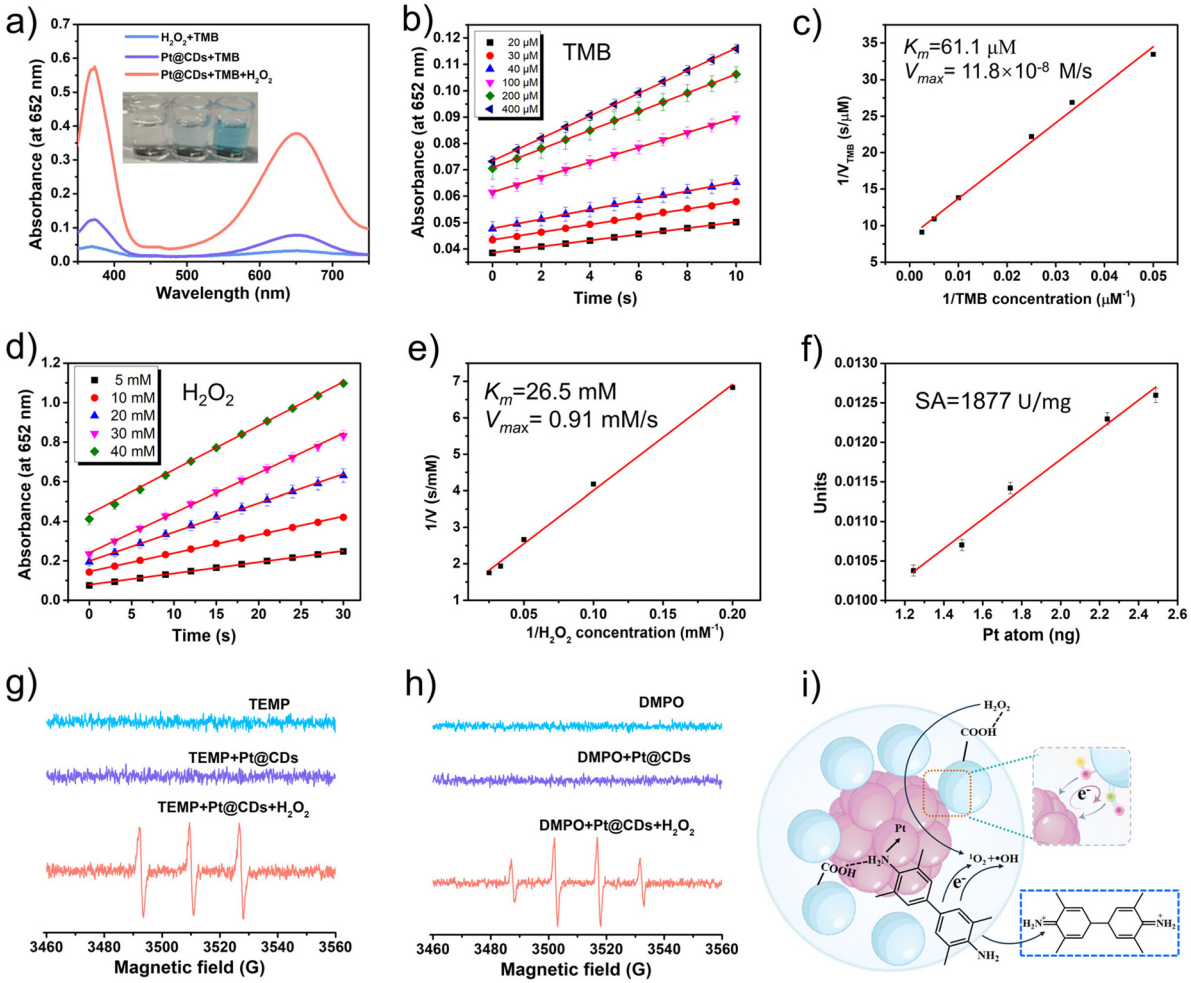

Fig. 2 The UV-vis spectra and photographs (inset) of H_2O_2 + TMB, TMB + Pt@CDs, and H_2O_2 + TMB + Pt@CDs (a); oxidation kinetics of TMB (b) and H_2O_2 (d) at different concentrations; Lineweaver–Burk double reciprocal plot of Pt@CDs with a fixed concentration of H_2O_2 or TMB *versus* different concentrations of TMB (c) or H_2O_2 (e); the specific activity of Pt@CDs was found to be 1877 U mg^{-1} (f); the ESR spectroscopy of Pt@CDs and the mixture of Pt@CDs and H_2O_2 by using TEMP (g) and DMPO (h) as trapping agents for $^1O_2$ and •OH, respectively; the schematic illustration of the Pt@CDs catalytic reaction and electron transfer process (i).

role in the binding to H_2O_2 due to the carboxyl groups acting as H_2O_2-binding sites.[55]

By using the nanozyme activity standardization method,[56] the POD specific activity of Pt@CDs was tested to be 1877 U mg^{-1} (Fig. 2g), 1860-fold higher than that of bovine serum albumin capped PtNPs (BSA-PtNPs, 1.009 U mg^{-1}).[34] Such high catalytic activity encouraged us to study their catalytic mechanism. Electron spin resonance (ESR) spectroscopy was performed to explore the POD-like catalysis process of Pt@CDs. 2,2,6,6-Tetramethyl-1-piperidine (TEMP) and 5,5-dimethyl-1-pyrroline N-oxide (DMPO) were used as trapping agents for singlet oxygen ($^1O_2$) and hydroxyl radicals (•OH), respectively. Compared with the negligible signal of Pt@CDs, the characteristic signals of DMPO-HO• and TEMP-$^1O_2$ adducts were observed (Fig. 2g and h) in the presence of H_2O_2, suggesting the production of •OH and $^1O_2$. Previous works have reported that Pt-based nanozymes can catalyse the generation of •OH or $^1O_2$.[53,57] Yet, reports on Pt-based nanozymes that catalyse the generation of •OH and $^1O_2$ simultaneously are rare. Two kinds of reactive oxygen species (ROS) generation are responsible for the enhanced POD-like activity of Pt@CDs. The proposed catalysis process of Pt@CDs is shown in Fig. 2i. H_2O_2 was adsorbed on the surface of Pt@CDs through hydrogen bonds with carboxyl groups of CDs,[55] while TMB bonds to Pt@CDs through coordination with PtNPs and electrostatic/hydrogen bonding with CDs. Then, H_2O_2 was activated and decomposed through the breaking of O–O or O–H bonds accompanied by the proton–electron transfer, resulting in the generation of •OH and $^1O_2$. The absorbed TMB on the surface of Pt@CDs was then oxidized by •OH and $^1O_2$, generating blue Ox-TMB as a product.

Furthermore, X-ray photoelectron spectroscopy (XPS) and Fourier transform infrared (FT-IR) spectroscopy were conducted to explore the combination between CDs and PtNPs. Our previous work demonstrated that the carbonyl groups located on the surface of CDs could be reduced to hydroxyl

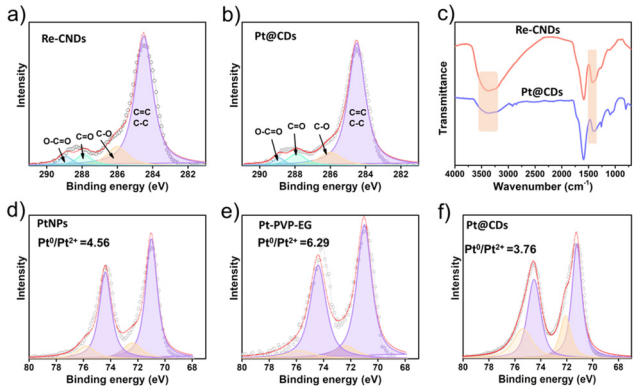

Fig. 3 The C 1s high-resolution XPS of Re-CDs (a) and Pt@CDs (b) with the analysis of peaks through curve fitting; the FT-IR spectra of Re-CDs and Pt@CDs (c); the Pt 4f high-resolution XPS with the analysis of peaks through curve fitting of PtNPs (d), Pt-PVP-EG (e), and Pt@CDs (f).

groups by $NaBH_4$.[49] As shown in Fig. S8† and Fig. 3a and b, C 1s XPS spectra of CDs, reduced CDs (Re-CDs) and Pt@CDs could be fitted with four peaks at 245.8, 260.0, 278.9 and 288.9 eV corresponding to the functional groups C═C/C–C, C–O, C═O, and COOH, respectively. All the structure contents were calculated and listed in Table S2.† It is evident that the carbonyl content decreased and the hydroxyl content increased in CDs after reduction by $NaBH_4$. In comparison to Re-CDs, the Pt@CDs exhibited a higher carbonyl content, indicating that the Pt@CD formation suppresses the reduction of CDs by $NaBH_4$. So, the carbonyl of CDs might coordinate with PtNPs, thereby facilitating the generation of PtNPs on the surface of CDs. As shown in Fig. 3c, it was observed that the absorption of O–H stretching and in-plane bending vibrations in the range of 3100–3500 cm^{-1} and 1430 cm^{-1}, respectively, significantly decreased in Pt@CDs compared to Re-CDs, suggesting the coordination between PtNPs and hydroxyl groups on the surface of CDs. The Pt 4f XPS were investigated to study the potential impact of CDs on the charge state of PtNPs. The Pt 4f7/2 and 4f5/2 exhibiting the binding energies of 71.2 and 74.5 eV, respectively, were attributed to Pt^0 while those of 72.1 and 75.4 eV were assigned to Pt^{2+}, suggesting that the Pt^{4+} ions were reduced to Pt^0 and Pt^{2+} by $NaBH_4$. As shown in Fig. 3d, the ratio of Pt^0 to Pt^{2+} in naked PtNPs was calculated to be 4.56. For PtNPs-PVP-EG, in which the surface of PtNPs was capped with PVP, the ratio of Pt^0 to Pt^{2+} increased to 6.29 (Fig. 3e), suggesting that capping PVP decreased the POD-like activity of the Pt nanozyme through increasing the Pt^0 ratio. In contrast, the ratio of Pt^0 to Pt^{2+} of Pt@CDs decreased to 3.76 (Fig. 3f), suggesting that CDs could regulate the charge state of the Pt nanozyme to achieve a suitable Pt^{2+} ratio.

Gao *et al.*[58] revealed that the charge transfer between the surface ligand and ruthenium (Ru) is the key factor in the improvement of the catalytic efficiency of Ru nanozymes. Li *et al.*[54] demonstrated that the charge states of Pt nanozyme are associated with the DNA templates. Our CDs have negligible POD-like activity, so the key electron/charge transfer process of POD-like activity is on the surface of the PtNPs or in the interface between PtNPs and CDs. For electron/charge transfer to occur, PtNPs need to accept or lose electrons. Pt^{2+} can coordinate with the TMB and the oxygen-containing groups on the surface of the CDs. The oxygen-containing groups of the CDs can combine with H_2O_2 and TMB through hydrogen bond and electrostatic interactions. So, the combination between Pt@CDs and the reaction substrate is promoted by Pt^{2+}, which ultimately accelerates the oxidation reaction of TMB by H_2O_2. In addition, Pt^{2+} can also accept electrons from TMB to form Pt^0, and the latter has better conductivity and can transfer electrons to H_2O_2, also accelerating the reaction. In conclusion, the presence of an appropriate amount of Pt^{2+} plays an important role in both substrate binding and electron/charge transfer processes. This facilitates the initiation and progression of the reaction, leading to Pt@CDs with enhanced POD enzyme activity. Hence, it can be speculated that both the hydroxyl and carbonyl groups of CDs have the potential to coordinate with Pt^{2+}, prompting the high stability and large Pt^{2+} ratio of Pt@CDs and then enhancing the POD-like activity. Similar to many nanozymes, the catalytic activity of Pt@CDs is dependent on pH and temperature, showing optimal catalytic activity at pH 3–5 and temperature of 25–45 °C (Fig. S9†). In addition, the influence of 19 kinds of metal ions on the POD-like activity of Pt@CDs was investigated. As displayed in Fig. S10,† Pt@CDs exhibited strong resistance to metal ions.

The colorimetric reaction of TMB catalysed by peroxidase mimics is often used for H_2O_2 sensing. Fig. 4a exhibits a typical H_2O_2 concentration-dependent colorimetric reaction using Pt@CDs to facilitate the oxidation of TMB by H_2O_2. The linear range is 5–500 μM (Fig. 4a, inset), and the LOD for H_2O_2 was 3.27 μM, lower than the allowable level of H_2O_2 specified by the US FDA (0.05 wt%, or 15 μM), suggesting the potential application of Pt@CDs in H_2O_2 detection in food products. The practical detection capability of the colorimetric sensor based on Pt@CDs was evaluated in both diluted orange juice and milk using the standard addition method. The assay yielded an acceptable relative standard deviation and recovery (%) for various concentrations of H_2O_2 detection, as shown in Tables S3 and S4.† These results demonstrated that the Pt@CD-based sensor is suitable for the detection of H_2O_2 in food products.

DA serves as a vital catecholamine neurotransmitter, playing a crucial role in regulating the central nervous, hormonal, and cardiovascular systems, as well as metabolism.[59] Since the degree of DA reflects the health status of organisms, a simple, rapid, and sensitive detection of DA is in high demand. Due to the reducibility, DA would induce the blue solution of Pt@CDs-H_2O_2-TMB to fade, leading to sensitive detection (Fig. 4b). The LOD and linear range of DA were 0.31 μM and 1–100 μM, respectively. Ascorbic acid (AA) is a common reducing agent that may interfere with DA detection. To eliminate the interference, we employed Cu^{2+} to mask AA since Cu^{2+} oxidizes AA but has no effect on DA. As shown in Fig. S11,† the absorbance variation of DA is much higher than that of AA even when the concentration of AA was 10 times

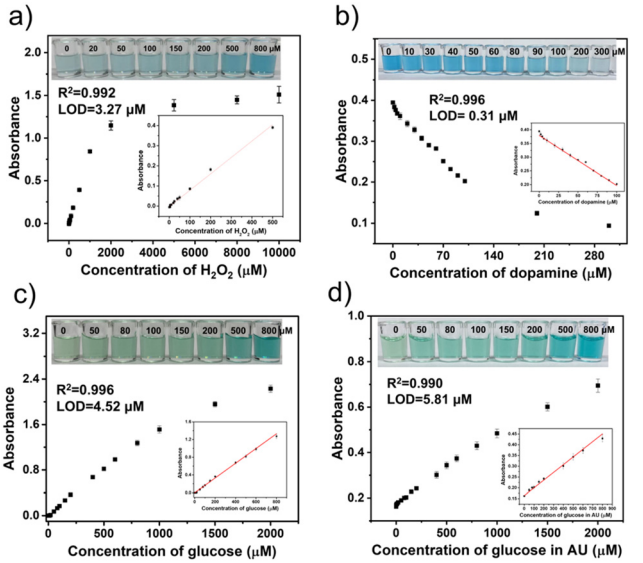

Fig. 4 Detection of H_2O_2 (a), and DA (b) by using Pt@CDs; detection of glucose in water (c) and AU (d) by combining Pt@CDs and GOx.

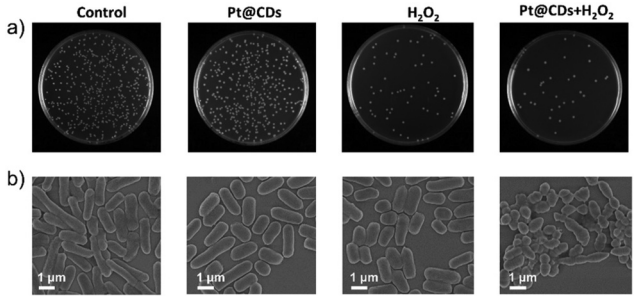

Fig. 5 The antibacterial activity (a), and SEM image (b) of Pt@CD nanozymes against *E. coli* that had been treated prior as control and after exposure to Pt@CDs, H_2O_2, and Pt@CDs + H_2O_2 as indicated. The concentrations of Pt@CDs and H_2O_2 were 7 μg mL^{-1} and 100 μM, respectively.

that of DA, suggesting that with the help of Cu^{2+}, the detection of DA is minimally affected by AA. The practical detection capability of the sensor based on Pt@CDs was evaluated in serum using the standard addition method. The obtained absorbance values were brought into the standard curve to calculate the DA concentration and the recovery (%). Table S5† showing satisfactory accuracy and precision for DA detection proved that the Pt@CD-based sensor could be applied for DA determination in real samples.

Glucose serves as the main energy source in biological systems, and disturbance in glucose concentration is frequently associated with a range of diseases such as hyperglycemia, diabetes and cancer.[60–62] Coupled with GOx, the POD-like activity of Pt@CDs can be extended for glucose detection. GOx facilitates the oxidation of glucose by dissolved O_2, producing H_2O_2 that could be detected using the colorimetric reaction of TMB catalysed by Pt@CDs. Therefore, the concentration of glucose could be determined. As shown in Fig. 4c, the absorbance of Ox-TMB was influenced by β-D-glucose concentrations. The linear range was 10–800 μM (Fig. 4c, inset) and the LOD was 4.52 μM. As shown in Fig. S12,† several glucose analogs including galactose, mannose, arabinose, fructose, and maltose with a considerable concentration of 10 or 5 mM only produced weak absorption variations while glucose introduced a high signal at a low concentration of 1 mM, indicating the high sensitivity and specificity of the detection assay here. To investigate the potential practical applications of the Pt@CDs-TMB system, detection of glucose in artificial urine (AU) sample was performed. As shown in Fig. 4d (top inset), with the increase in glucose concentration, the absorbance signals of the solution gradually increased with a visual detection concentration of 50 μM. The relationship between absorbance and glucose concentration is displayed, covering a range of 0–2000 μM, as shown in Fig. 4d. A calibration plot with a high correlation coefficient (R^2) of 0.990 and a broad linear range of 10–800 μM could be extracted (Fig. 4d, inset). The LOD of glucose in AU was calculated to be 5.81 μM.

The capability of Pt@CDs to generate •OH and $^1O_2$ inspired us to utilize them as an antibacterial agent. The antibacterial activity of Pt@CDs against *E. coli.* was explored. As displayed in Fig. 5a, Pt@CDs did not inhibit the growth of *E. coli.*, while H_2O_2 exhibited antibacterial performance. Notably, the antibacterial activity of H_2O_2 was significantly enhanced in the presence of Pt@CDs. For understanding the antibacterial mechanism of the Pt@CDs-H_2O_2 system, a scanning electron microscope (SEM) was used to observed the membrane morphologies of *E. coli.* As shown in Fig. 5b, the *E. coli.* cells treated with individual Pt@CDs or H_2O_2 presented the rod-like shape, and the cell membrane was smooth and undamaged. In contrast, after the treatment with both Pt@CDs and H_2O_2, the *E. coli.* cells became shorter and the cell membrane turned into a rough structure, adhered to each other, or even destroyed. The results indicated that H_2O_2 could inhibit the reproduction of bacteria while Pt@CDs can destroy the cell membrane in the presence of H_2O_2. The bacteriostasis rate of Pt@CDs + H_2O_2 reached 91%, suggesting a better bactericidal effect with the assistance of Pt@CDs.

Experimental

Preparation of Pt@CDs

160 μL of CDs (10 mg mL^{-1}), 1.73 mL of water, and chloroplatinic acid (40 mM, 50 μL) were added into a vial under stirring. After 10 min, 60 μL of NaOH solution (1 M) was added. After stirring for about 10 min, $NaBH_4$ solution (10 mg mL^{-1}, 3 mL) was added. Then, the solution was stirred for another 3 h and stood overnight. The resulting solution containing Pt@CDs was neutralized with HCl (1 M, about 700 μL) and filtered using 0.22 μm BIOSHARP membrane filters. Meanwhile, naked PtNPs and PtNPs-PVP were prepared by replacing CDs with water and PVP with the total dose of 1.6 mg.

POD-like catalytic activity of Pt@CDs

The POD-like catalytic activity of Pt@CDs was evaluated by measuring the oxidation of TMB in the presence of H_2O_2. Typically, 50 μL of H_2O_2 (2 mM in 0.33 M sodium acetate and 0.0166 M citric acid (buffer A for short)), 50 μL of TMB (2 mM in 1 mM ethylenediaminetetraacetic acid disodium salt and 9.8 mM citric acid (buffer B for short)) and 2.5 μL of Pt@CDs were mixed at room temperature and incubated for a certain time. POD-like catalytic activity was measured using the absorbance at 652 nm on a plate reader. Repeatability of the experiment was confirmed based on the averaged values of three repeated measurements. In the control experiments, 50 μL of ABTS, OPD, or DAB (2 mM in buffer B) were added to the mixture instead of TMB.

H_2O_2 detection using Pt@CDs

50 μL of TMB (2 mM in buffer B), 50 μL of H_2O_2 (different concentrations in buffer A) and 2.5 μL of Pt@CDs were mixed and incubated at 40 °C for 10 min. The reaction was analysed by the observation of absorbance at 652 nm. The detection was repeated 3 times for the averaged value.

Glucose detection using GOx and Pt@CDs

The detection of glucose was carried out as follows: 5 μL of 50 mg mL^{-1} GOx and 50 μL of glucose at various concentrations in buffer A were incubated 30 min at 37 °C. Then, 50 μL of TMB (2 mM in buffer B) and 2.5 μL of Pt@CDs were added to the above reaction solution. Next, the mixture was placed in an incubator at a temperature of 37 °C for a duration of 20 min. Absorbance at 652 nm was measured. In control experiments, galactose, mannose, arabinose, and fructose at a concentration of 10 mM and maltose at a concentration of 5 mM were chosen to verify the selectivity for glucose.

Antibacterial activity of Pt@CDs

A single colony of *E. coli* DH 5α from solid agar plates was cultured in liquid Luria–Bertani (LB) medium at 37 °C for 12 h. Then, the medium was diluted 10^2-fold and cultured for 3 h more until the OD600 reached 0.45 (10^7 cfu mL^{-1}). Then, different groups involving PBS, Pt@CDs, H_2O_2 (100 μM), and Pt@CDs + H_2O_2 were added to 500 μL of 10^3-diluted bacterial cells. The mixture was shook at 37 °C and 180 rpm for 3 h. Finally, the obtained bacterial solution was diluted 10^2-fold and plated onto agar plates for 24-h incubation at 37 °C. 6 plates were prepared for each sample to minimize errors.

Conclusion

In summary, we designed a Pt@CDs hybrid nanozyme by growing "naked" PtNPs directly on the surface of CDs through an *in situ* process. Both hydroxyl and carbonyl groups of CDs could coordinate with Pt^{2+}, prompting the high stability and large Pt^{2+} ratio of Pt@CDs and subsequently enhancing the POD-like activity. CDs could bind with H_2O_2 and TMB through hydrogen bonds and electrostatic forces. Hence, the Pt@CDs exhibit remarkable POD-like activity, with a specific activity of 1877 U mg^{-1} and high affinity to TMB and H_2O_2. Based on this POD-like activity, Pt@CDs were employed for the colorimetric detection of H_2O_2 and DA. Combining with GOx, a colorimetric glucose detection assay was established and the LOD was 5.8 μM with a linear range of 10–800 μM in AU. Moreover, the Pt@CDs showed an H_2O_2-involving bactericidal effect that could destroy the bacterial cell membrane. Our findings provide new opportunities for designing hybrid nanozymes with good colloidal stability and high catalytic activity using CDs as nucleating templates and stabilizers, promoting the design and application of hybrid nanozymes.

Author contributions

Cui Liu: conceptualization, methodology, investigation, data curation, and writing – original draft preparation. Jiao Hu: conceptualization, methodology, and validation. Wenwen Yang: methodology and validation. Jinyu Shi: methodology. Yiming Chen: validation. Xing Fan: methodology. Wenhui Gao: methodology and validation. Liangliang Cheng: methodology and validation. Qing-Ying Luo: writing – reviewing and editing. Mingzhen Zhang: writing – reviewing and editing.

Conflicts of interest

There are no conflicts to declare.

Acknowledgements

This work was supported by the National Natural Science Foundation of China (32171392, 82000523, 22174053, and 21805021), the China Postdoctoral Science Foundation (2020M683449), the Guangdong Foundation for Basic and Applied Research (2021A1515010300), the Natural Science Foundation of Shaanxi province (2021JQ-009, 2020JQ-095), the high level discipline cultivation project of Shenzhen Polytechnic University, and the "Young Talent Support Plan" of Xi'an Jiaotong University, China (No. YX6J001). We also thank Dr Zijun Ren at the Instrument Analysis Center of Xi'an Jiaotong University for assisting with TEM analysis.

References

1 Y. Huang, J. Ren and X. Qu, Nanozymes: Classification, Catalytic Mechanisms, Activity Regulation, and Applications, *Chem. Rev.*, 2019, **119**(6), 4357–4412.
2 L. H. Posorske, Industrial-Scale Application of Enzymes to the Fats and Oil Industry, *J. Am. Oil Chem. Soc.*, 1984, **61**(11), 1758–1760.
3 M. Choct, Enzymes for the feed industry: past, present and future, *Worlds Poult. Sci. J.*, 2006, **62**(1), 5–15.

4 A. Abuchowski, G. M. Kazo, C. R. Verhoest, T. Vanes, D. Kafkewitz, M. L. Nucci, A. T. Viau and F. F. Davis, Cancer-Therapy with Chemically Modified Enzymes .1. Antitumor Properties of Polyethylene Glycol-Asparaginase Conjugates, *Cancer Biochem. Biophys.*, 1984, **7**(2), 175–186.
5 X. Li, L. Wang, D. Du, L. Ni, J. Pan and X. Niu, Emerging applications of nanozymes in environmental analysis: Opportunities and trends, *TrAC, Trends Anal. Chem.*, 2019, **120**, 115653.
6 L. Gao, J. Zhuang, L. Nie, J. Zhang, Y. Zhang, N. Gu, T. Wang, J. Feng, D. Yang, S. Perrett and X. Yan, Intrinsic peroxidase-like activity of ferromagnetic nanoparticles, *Nat. Nanotechnol.*, 2007, **2**(9), 577–583.
7 F. Natalio, R. Andre, A. F. Hartog, B. Stoll, K. P. Jochum, R. Wever and W. Tremel, Vanadium pentoxide nanoparticles mimic vanadium haloperoxidases and thwart biofilm formation, *Nat. Nanotechnol.*, 2012, **7**(8), 530–535.
8 W. Zhang, S. Hu, J.-J. Yin, W. He, W. Lu, M. Ma, N. Gu and Y. Zhang, Prussian Blue Nanoparticles as Multienzyme Mimetics and Reactive Oxygen Species Scavengers, *J. Am. Chem. Soc.*, 2016, **138**(18), 5860–5865.
9 J. Lee, H. Liao, Q. Wang, J. Han, J.-H. Han, H. E. Shin, M. Ge, W. Park and F. Li, Exploration of nanozymes in viral diagnosis and therapy, *Exploration*, 2022, **2**(1), 20210086.
10 G. Tang, J. He, J. Liu, X. Yan and K. Fan, Nanozyme for tumor therapy: Surface modification matters, *Exploration*, 2021, **1**(1), 75–89.
11 Y. Zhao, Z. Zhang, Z. Pan and Y. Liu, Advanced bioactive nanomaterials for biomedical applications, *Exploration*, 2021, **1**(3), 20210089.
12 Q. Yang, Y.-Y. Mao, Q. Liu and W.-W. He, Metal nanozymes with multiple catalytic activities: regulating strategies and biological applications, *Rare Met.*, 2023, **42**(9), 2928–2948.
13 J. Wu, X. Wang, Q. Wang, Z. Lou, S. Li, Y. Zhu, L. Qin and H. Wei, Nanomaterials with enzyme-like characteristics (nanozymes): next-generation artificial enzymes (II), *Chem. Soc. Rev.*, 2019, **48**(4), 1004–1076.
14 Y. Zhou, B. Liu, R. Yang and J. Liu, Filling in the Gaps between Nanozymes and Enzymes: Challenges and Opportunities, *Bioconjugate Chem.*, 2017, **28**(12), 2903–2909.
15 J. Zhao, H. Wang, H. Geng, Q. Yang, Y. Tong and W. He, Au/N-Doped Carbon Dot Nanozymes as Light-Controlled Anti- and Pro-Oxidants, *ACS Appl. Nano Mater.*, 2021, **4**(7), 7253–7263.
16 H. Qiu, F. Pu, X. Ran, C. Liu, J. Ren and X. Qu, Nanozyme as Artificial Receptor with Multiple Readouts for Pattern Recognition, *Anal. Chem.*, 2018, **90**(20), 11775–11779.
17 L. Tian, J. Qi, O. Oderinde, C. Yao, W. Song and Y. Wang, Planar intercalated copper(II) complex molecule as small molecule enzyme mimic combined with Fe_3O_4 nanozyme for bienzyme synergistic catalysis applied to the microRNA biosensor, *Biosens. Bioelectron.*, 2018, **110**, 110–117.
18 J. Zhao, J. Gong, J. Wei, Q. Yang, G. Li, Y. Tong and W. He, Metal organic framework loaded fluorescent nitrogen-doped carbon nanozyme with light regulating redox ability for detection of ferric ion and glutathione, *J. Colloid Interface Sci.*, 2022, **618**, 11–21.
19 Y. Huang, X. Ran, Y. Lin, J. Ren and X. Qu, Self-assembly of an organic-inorganic hybrid nanoflower as an efficient biomimetic catalyst for self-activated tandem reactions, *Chem. Commun.*, 2015, **51**(21), 4386–4389.
20 L. Gao and X. Yan, Nanozymes: an emerging field bridging nanotechnology and biology, *Sci. China: Life Sci.*, 2016, **59**(4), 400–402.
21 D. Duan, K. Fan, D. Zhang, S. Tan, M. Liang, Y. Liu, J. Zhang, P. Zhang, W. Liu, X. Qiu, G. P. Kobinger, G. F. Gao and X. Yan, Nanozyme-strip for rapid local diagnosis of Ebola, *Biosens. Bioelectron.*, 2015, **74**, 134–141.
22 Y.-Y. Huang, Y.-H. Lin, F. Pu, J.-S. Ren and X.-G. Qu, The Current Progress of Nanozymes in Disease Treatments, *Prog. Biochem. Biophys.*, 2018, **45**(2), 256–267.
23 B.-W. Yang, Y. Chen and J.-L. Shi, Nanozymes in Catalytic Cancer Theranostics, *Prog. Biochem. Biophys.*, 2018, **45**(2), 237–255.
24 J. Niu, Y. Sun, F. Wang, C. Zhao, J. Ren and X. Qu, Photomodulated Nanozyme Used for a Gram-Selective Antimicrobial, *Chem. Mater.*, 2018, **30**(20), 7027–7033.
25 J. Wu, S. Li and H. Wei, Integrated nanozymes: facile preparation and biomedical applications, *Chem. Commun.*, 2018, **54**(50), 6520–6530.
26 W. Li, Z. Liu, C. Liu, Y. Guan, J. Ren and X. Qu, Manganese Dioxide Nanozymes as Responsive Cytoprotective Shells for Individual Living Cell Encapsulation, *Angew. Chem., Int. Ed.*, 2017, **56**(44), 13661–13665.
27 C. Liu, W. Fan, W.-X. Cheng, Y. Gu, Y. Chen, W. Zhou, X.-F. Yu, M. Chen, M. Zhu, K. Fan and Q.-Y. Luo, Red Emissive Carbon Dot Superoxide Dismutase Nanozyme for Bioimaging and Ameliorating Acute Lung Injury, *Adv. Funct. Mater.*, 2023, **33**(19), 2213856.
28 W. Gao, J. He, L. Chen, X. Meng, Y. Ma, L. Cheng, K. Tu, X. Gao, C. Liu, M. Zhang, K. Fan, D.-W. Pang and X. Yan, Deciphering the catalytic mechanism of superoxide dismutase activity of carbon dot nanozyme, *Nat. Commun.*, 2023, **14**(1), 160.
29 A. Lin, Z. Sun, X. Xu, S. Zhao, J. Li, H. Sun, Q. Wang, Q. Jiang, H. Wei and D. Shi, Self-Cascade Uricase/Catalase Mimics Alleviate Acute Gout, *Nano Lett.*, 2022, **22**, 508–516.
30 R. Chen, X. Chen, Y. Zhou, T. Lin, Y. Leng, X. Huang and Y. Xiong, "Three-in-One" Multifunctional Nanohybrids with Colorimetric Magnetic Catalytic Activities to Enhance Immunochromatographic Diagnosis, *ACS Nano*, 2022, **16**(2), 3351–3361.
31 H. Wang, J. Zhao, C. Liu, Y. Tong and W. He, Pt Nanoparticles Confined by Zirconium Metal-Organic Frameworks with Enhanced Enzyme-like Activity for Glucose Detection, *ACS Omega*, 2021, **6**(7), 4807–4815.
32 J. M. An, Y. Ju, J. H. Kim, H. Lee, Y. Jung, J. Kim, Y. J. Kim, J. Kim and D. Kim, A metastasis suppressor Pt-dendrimer nanozyme for the alleviation of glioblastoma, *J. Mater. Chem. B*, 2021, **9**(19), 4015–4023.

33 Y. Park, P. K. Gupta, V.-K. Tran, S. E. Son, W. Hur, H. B. Lee, J. Y. Park, S. N. Kim and G. H. Seong, PVP-stabilized PtRu nanozymes with peroxidase-like activity and its application for colorimetric and fluorometric glucose detection, *Colloids Surf., B*, 2021, **204**, 111783.
34 S.-B. He, R.-T. Chen, Y.-Y. Wu, G.-W. Wu, H.-P. Peng, A.-L. Liu, H.-H. Deng, X.-H. Xia and W. Chen, Improved enzymatic assay for hydrogen peroxide and glucose by exploiting the enzyme-mimicking properties of BSA-coated platinum nanoparticles, *Microchim. Acta*, 2019, **186**(12), 778.
35 L. Chen, N. Wang, X. Wang and S. Ai, Protein-directed in situ synthesis of platinum nanoparticles with superior peroxidase-like activity, and their use for photometric determination of hydrogen peroxide, *Microchim. Acta*, 2013, **180**(15), 1517–1522.
36 W. Li, B. Chen, H. Zhang, Y. Sun, J. Wang, J. Zhang and Y. Fu, BSA-stabilized Pt nanozyme for peroxidase mimetics and its application on colorimetric detection of mercury(II) ions, *Biosens. Bioelectron.*, 2015, **66**, 251–258.
37 J. Fan, J.-J. Yin, B. Ning, X. Wu, Y. Hu, M. Ferrari, G. J. Anderson, J. Wei, Y. Zhao and G. Nie, Direct evidence for catalase and peroxidase activities of ferritin–platinum nanoparticles, *Biomaterials*, 2011, **32**(6), 1611–1618.
38 Y. Wang, C. He, W. Li, J. Zhang and Y. Fu, Catalytic Performance of Oligonucleotide-Templated Pt Nanozyme Evaluated by Laccase Substrates, *Catal. Lett.*, 2017, **147**(8), 2144–2152.
39 X. Li, Q. Huang, W. Li, J. Zhang and Y. Fu, N-Acety-L-Cysteine-Stabilized, Pt Nanozyme for Colorimetric Assay of Heparin, *J. Anal. Test.*, 2019, **3**(3), 277–285.
40 S. E. Son, P. K. Gupta, W. Hur, H. B. Lee, Y. Park, J. Park, S. N. Kim and G. H. Seong, Citric Acid-Functionalized Rhodium-Platinum Nanoparticles as Peroxidase Mimics for Determination of Cholesterol, *ACS Appl. Nano Mater.*, 2021, **4**(8), 8282–8291.
41 Y.-L. Dong, H.-G. Zhang, Z. U. Rahman, L. Su, X.-J. Chen, J. Hu and X.-G. Chen, Graphene oxide–Fe_3O_4 magnetic nanocomposites with peroxidase-like activity for colorimetric detection of glucose, *Nanoscale*, 2012, **4**(13), 3969–3976.
42 Y. Tao, Y. Lin, Z. Huang, J. Ren and X. Qu, Incorporating Graphene Oxide and Gold Nanoclusters: A Synergistic Catalyst with Surprisingly High Peroxidase-Like Activity Over a Broad pH Range and its Application for Cancer Cell Detection, *Adv. Mater.*, 2013, **25**(18), 2594–2599.
43 L. Gong, Y. Chen, X. Bai, T. Xu, S. Wu, W. Song and X. Feng, Peroxidase-mimicking Pt nanodots supported on polymerized ionic liquid wrapped multi-walled carbon nanotubes for colorimetric detection of hydrogen peroxide and glucose, *Microchem. J.*, 2021, **163**, 105872.
44 S. Y. Lim, W. Shen and Z. Gao, Carbon Quantum Dots and Their Applications, *Chem. Soc. Rev.*, 2015, **44**(1), 362–381.
45 F. Yuan, S. Li, Z. Fan, X. Meng, L. Fan and S. Yang, Shining Carbon Dots: Synthesis and Biomedical and Optoelectronic Applications, *Nano Today*, 2016, **11**(5), 565–586.
46 C. Ding, A. Zhu and Y. Tian, Functional Surface Engineering of C-Dots for Fluorescent Biosensing and in Vivo Bioimaging, *Acc. Chem. Res.*, 2014, **47**(1), 20–30.
47 J. C. G. Esteves Da Silva and H. M. R. Goncalves, Analytical and bioanalytical applications of carbon dots, *TrAC, Trends Anal. Chem.*, 2011, **30**(8), 1327–1336.
48 Y. Zhang, W. Gao, Y. Ma, L. Cheng, L. Zhang, Q. Liu, J. Chen, Y. Zhao, K. Tu, M. Zhang and C. Liu, Integrating Pt nanoparticles with carbon nanodots to achieve robust cascade superoxide dismutase-catalase nanozyme for antioxidant therapy, *Nano Today*, 2023, **49**, 101768.
49 C. Liu, L. Bao, M. Yang, S. Zhang, M. Zhou, B. Tang, B. Wang, Y. Liu, Z.-L. Zhang, B. Zhang and D.-W. Pang, Surface Sensitive Photoluminescence of Carbon Nanodots: Coupling between the Carbonyl Group and π-Electron System, *J. Phys. Chem. Lett.*, 2019, **10**, 3621–3629.
50 M. Yang, C. Liu, Y. Peng, R.-Z. Xiao, S. Zhang, Z.-L. Zhang, B. Zhang and D.-W. Pang, Surface chemistry tuning the selectivity of carbon nanodots towards Hg2+ recognition, *Anal. Chim. Acta*, 2021, **1146**, 33–40.
51 J. Chen, T. Herricks, M. Geissler and Y. Xia, Single-Crystal Nanowires of Platinum Can Be Synthesized by Controlling the Reaction Rate of a Polyol Process, *J. Am. Chem. Soc.*, 2004, **126**(35), 10854–10855.
52 Y. Chen, P. Wang, H. Hao, J. Hong, H. Li, S. Ji, A. Li, R. Gao, J. Dong, X. Han, M. Liang, D. Wang and Y. Li, Thermal Atomization of Platinum Nanoparticles into Single Atoms: An Effective Strategy for Engineering High-Performance Nanozymes, *J. Am. Chem. Soc.*, 2021, **143**(44), 18643–18651.
53 M. J. Liang, Y. B. Wang, K. Ma, S. S. Yu, Y. Y. Chen, Z. Deng, Y. Liu and F. Wang, Engineering Inorganic Nanoflares with Elaborate Enzymatic Specificity and Efficiency for Versatile Biofilm Eradication, *Small*, 2020, **16**(41), 2002348.
54 Y. Fu, X. Zhao, J. Zhang and W. Li, DNA-Based Platinum Nanozymes for Peroxidase Mimetics, *J. Phys. Chem. C*, 2014, **118**(31), 18116–18125.
55 H. J. Sun, A. D. Zhao, N. Gao, K. Li, J. S. Ren and X. G. Qu, Deciphering a Nanocarbon-Based Artificial Peroxidase: Chemical Identification of the Catalytically Active and Substrate-Binding Sites on Graphene Quantum Dots, *Angew. Chem., Int. Ed.*, 2015, **54**(24), 7176–7180.
56 B. Jiang, D. Duan, L. Gao, M. Zhou, K. Fan, Y. Tang, J. Xi, Y. Bi, Z. Tong, G. F. Gao, N. Xie, A. Tango, G. Nie, M. Liang and X. Yan, Standardized assays for determining the catalytic activity and kinetics of peroxidase-like nanozymes, *Nat. Protoc.*, 2018, **13**(7), 1506–1520.
57 P. Jin, X. Niu, Z. Gao, X. Xue, F. Zhang, W. Cheng, C. Ren, H. Du, A. Manyande and H. Chen, Ultrafine Platinum Nanoparticles Supported on Covalent Organic Frameworks As Stable and Reusable Oxidase-Like Catalysts for Cellular Glutathione Detection, *ACS Appl. Nano Mater.*, 2021, **4**(6), 5834–5841.
58 H. Fan, J. Zheng, J. Xie, J. Liu, X. Gao, X. Yan, K. Fan and L. Gao, Surface Ligand Engineering Ruthenium Nanozyme

Superior to Horseradish Peroxidase for Enhanced Immunoassay, *Adv. Mater.*, 2023, 2300387.

59 M. N. Ivanova, E. D. Grayfer, E. E. Plotnikova, L. S. Kibis, G. Darabdhara, P. K. Boruah, M. R. Das and V. E. Fedorov, Pt-Decorated Boron Nitride Nanosheets as Artificial Nanozyme for Detection of Dopamine, *ACS Appl. Mater. Interfaces*, 2019, **11**(25), 22102–22112.

60 M. W. Schwartz, R. J. Seeley, M. H. Tschöp, S. C. Woods, G. J. Morton, M. G. Myers and D. D'Alessio, Cooperation between brain and islet in glucose homeostasis and diabetes, *Nature*, 2013, **503**(7474), 59–66.

61 B. Uestuenel, K. Friedrich, A. Maida, X. Wang, A. Krones-Herzig, O. Seibert, A. Sommerfeld, A. Jones, T. P. Sijmonsma, C. Sticht, N. Gretz, T. Fleming, P. P. Nawroth, W. Stremmel, A. J. Rose, M. Berriel-Diaz, M. Blüher and S. Herzig, Control of diabetic hyperglycaemia and insulin resistance through TSC22D4, *Nat. Commun.*, 2016, **7**(1), 13267.

62 E. Giovannucci, D. M. Harlan, M. C. Archer, R. M. Bergenstal, S. M. Gapstur, L. A. Habel, M. Pollak, J. G. Regensteiner and D. Yee, Diabetes and Cancer: A consensus report, *Diabetes Care*, 2010, **33**(7), 1674–1685.